Multivariate control charts for calibration of hydrophones using the Mahalanobis distance

Steven E. Crocker[1] and William H. Slater[2]

[1]Naval Undersea Warfare Center Division, Newport, RI 02841, USA
[2]Naval Undersea Warfare Center Division, Newport, RI 02841, USA

William H. Slater
Naval Undersea Warfare Center Division Newport
1176 Howell Street
Newport, RI 02841, USA
william.h.slater.civ@us.navy.mil

Abstract: *Statistical analysis of data to ensure the validity of calibrations can be challenged when the measurement model describes a process and result that spans a high-dimensional parameter space. Calibration of hydrophones presents one such case whereby the sensitivity to acoustic pressure is calculated using measured values for several different quantities and the result is needed at many excitation frequencies distributed over a large bandwidth. To address this challenge, a multivariate statistical analysis procedure was developed that supports efficient and effective process control for hydrophone calibrations. It first characterizes the in-control condition by the mean and covariance of measurements expressed in a p-dimensional parameter space using a curated training data set. The procedure then tests subsequent measurements against a control limit using Hotelling's T^2-test to compare the current measurement process to the training data. A case study for free-field calibration of hydrophones spanning a frequency range of 1 kHz to 200 kHz is described. An emergent defect in a measuring instrument was detected by inspection of data presented in a multivariate control chart, thus helping to ensure the validity of calibration results reported in certificates issued by the laboratory.*

Keywords: *hydrophone calibration, multivariate control chart, Mahalanobis distance*

1. INTRODUCTION

Calibration laboratories that perform to the requirements of International Standard ISO/IEC 17025:2017 [1] employ processes to ensure the validity of their measurement results. Among these is the collection and statistical analysis of data such that trends are detectable. Specific monitoring techniques described in the standard include functional checks of measuring equipment and use of control charts. For high-volume services, it is advantageous to integrate these statistical control processes directly into the calibration procedure to provide efficient, responsive and cost-effective service to the laboratory's clients.

Employment of statistical process controls using the classic application of Shewhart [2] control charts in a calibration laboratory can present challenges not encountered in other settings. First, when the product is a measurement, its value may not known in advance. Second, the measurement may be required for a large number of auxiliary parameters. For example, a hydrophone response can vary with the frequency of the measured sound, and it is not practicable to employ a Shewhart control chart to monitor the calibration process at hundreds of discrete frequencies.

The problem of statistical process control for frequency dependent transducer (e.g., hydrophone) calibrations has a useful analogue in the chemical process industry. Industrial chemical processing requires that controls are applied prior to the availability of the final manufactured product and related to product quality by a known process model [3]. In a hydrophone calibration where the true sensitivity is unknown prior to measurement, it is also necessary to monitor and respond to intermediate process variables that influence the calibration result according to a known measurement model. Chemical processing also requires monitoring of a large number of intermediate process variables, applying methods to reduce the dimensionality of the parameter space and identify an out-of-control condition based on evaluating a single statistic [4]. Such reduction of dimensionality can also be used to create a single statistic for transducer measurements performed at hundreds of frequencies.

The U.S. Navy's Underwater Sound Reference Division (USRD) developed methods to address the challenges of 1) the inability to apply process controls directly to the calibration result itself, 2) the high-dimensional parameter space spanned by intermediate variables observed during the calibration measurements, and 3) the need for controls integrated directly and continuously into the calibration procedure for minimal disruption of a high-volume process. Section 2 reviews the general theory for statistical analysis of a process using control charts. The *Mahalanobis distance* [5] is introduced as an effective measure used to evaluate whether a given multivariate process is *in control* or *out of control*. Section 3 reviews free-field methods for the relative calibration of acoustic transducers [6]. The electrical transfer impedance between a hydrophone and an acoustic projector is posed as a good candidate for process monitoring. Section 4 reports a case study in which the statistical process controls described here were successfully applied to one of the laboratory's calibration services. Section 5 concludes with a brief summary.

2. CONTROL CHART THEORY

Construction of a control chart to monitor a single material property or process parameter begins with repeated measurements of a material property or parameter when the process is stable. The measurements are performed over a period of time sufficient to observe all sources

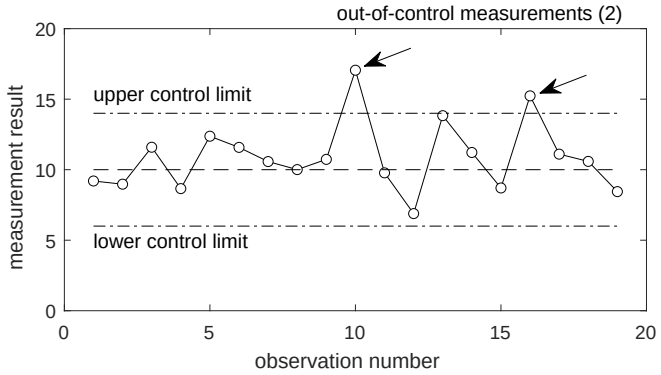

Figure 1: Shewhart control chart example

of variability intrinsic to the process. The results are used to determine the tolerable variation and will serve as a reference for future quality control analyses applied to that same material property or process parameter.

The well-established Shewhart [2] control chart is generated by defining a central line with a value equal to the mean of the initial measurements (i.e., training data) along with upper and lower control limits, defining the range of values for which the process is said to be *in control*. Once the control chart is established, process data continues to be collected and is plotted onto the chart over time as illustrated in Fig. 1. Measured data that remains within the control limits exemplifies a process that remains *in control*. However, when measured data lies outside the control limits, or develops trends that show systematic bias with respect to the central line, then the system is said to be *out of control* and actions stipulated in applicable quality procedures are taken.

These one-dimensional methods are not suited to processes where a vector $\boldsymbol{z}_i$ emerges from the analysis expressing values of several measured properties. In response, applications for control charts have been extended by the development of statistical methods to control processes that require the analysis of multivariate data sets characterized by mutual correlations among the quantities measured [7]. Multivariate statistical techniques frequently employ the distance between vector-valued objects to represent a process; the Euclidean and Mahalanobis distances being the most common [8]. The Mahalanobis distance has the advantage of being computed using the covariance matrix of the data set under consideration, thus properly accounting for correlation in the data.

Processes subjected to statistical controls contain random errors that tend toward a normal distribution as the number of measurements increases. The multivariate form of the probability density function of the normal distribution for a vector quantity $\boldsymbol{z}_i$ is

$$f(\boldsymbol{z}_i) = \frac{\exp\left[-\frac{1}{2}(\boldsymbol{z}_i - \boldsymbol{\mu})\mathbf{C}^{-1}(\boldsymbol{z}_i - \boldsymbol{\mu})^{\mathrm{T}}\right]}{|\mathbf{C}|^{1/2}\,(2\pi)^{p/2}}, \tag{1}$$

where $\boldsymbol{\mu}$ is the true mean vector ($1 \times p$) of $\boldsymbol{z}_i$, $\mathbf{C}$ is its true covariance matrix ($p \times p$), and T is the transpose operator.

Locations in a p-dimensional space having equal density are found by taking the natural logarithm of (1), so that rearrangement yields the Mahalanobis distance

$$D_i^2 = (\boldsymbol{z}_i - \boldsymbol{\mu})\mathbf{C}^{-1}(\boldsymbol{z}_i - \boldsymbol{\mu})^{\mathrm{T}} = a \text{ (constant)} \tag{2}$$

which has the χ^2-distribution with p-degrees of freedom. The 100α percentage of the vectors $\boldsymbol{z}_i$,

$$(\boldsymbol{z}_i - \boldsymbol{\mu})\,\mathbf{C}^{-1}\,(\boldsymbol{z}_i - \boldsymbol{\mu})^{\mathrm{T}} \leq \chi_\alpha^2(p), \tag{3}$$

is an inequality that describes a p-dimensional ellipsoid. However, when the true values of $\boldsymbol{\mu}$ and $\mathbf{C}$ are not known, the Mahalanobis distance D^2 must instead be computed using the estimates $\hat{\boldsymbol{\mu}}$ and $\hat{\mathbf{C}}$

$$D_i^2 = (\boldsymbol{z}_i - \hat{\boldsymbol{\mu}})\hat{\mathbf{C}}^{-1}(\boldsymbol{z}_i - \hat{\boldsymbol{\mu}})^{\mathrm{T}} \leq T_\alpha^2(p, n), \tag{4}$$

where the χ^2-distribution was replaced with Hotelling's T^2-distribution.

When used in Hotelling's T^2-test, the Mahalanobis distance D^2 is a powerful tool to build multivariate process control charts [9]. The confidence limits are established using a training data set which ought to contain measurements representing the normal, in-control situation including all sources of variability. Therefore, the training set itself must first be cleared of outliers. To accomplish this, the Mahalanobis distance between each observation $\boldsymbol{z}_i$ and the mean vector $\boldsymbol{\mu}$ is computed using (4) and compared to the critical T_α^2-value

$$T_\alpha^2\,(p, n) \approx \frac{(n-1)^2}{n}\beta_{(\alpha;p/2,(n-p-1)/2)}. \tag{5}$$

Limits established with the β-distribution account for the fact that $\boldsymbol{\mu}$ and $\mathbf{C}$ are unknown, and that detection of outliers is retrospective. One or more measurements may thus be deleted from the training data and those that remain used to calculate the mean vector $\hat{\boldsymbol{\mu}}$ and covariance matrix $\hat{\mathbf{C}}$ estimates.

After clearing outliers from the training data, the Mahalanobis distances are recomputed and the upper control limit T_{u}^2 used to predict whether new observations are *in-control* or not, as determined by

$$T_{\mathrm{u}}^2\,(p, n) = \frac{p(n-1)(n+1)}{n(n-p)}F_{(\alpha;p,(n-p))}. \tag{6}$$

The Mahalanobis distance (4) of each subsequent measurement vector $\boldsymbol{z}_i$ can then be plotted together with the control limit T_{u}^2 to obtain a multivariate control chart. Actions taken when the control limit is exceeded, and the process is determined to be *out-of-control*, are prescribed in the laboratory's quality control procedures.

3. HYDROPHONE MEASUREMENT MODEL FOR PROCESS CONTROL

This section identifies a process and candidate parameter for process monitoring, $|Z_{\mathrm{PR}}|$, by combining methods to calibrate hydrophones and measure the candidate parameter without compromising quality or throughput. The resulting calibration conforms to IEC 60565-1:2020 [6] while generating data for process monitoring as required by ISO/IEC 17025:2017 [1].

The process comprises

(i) calibration of the projector P using a calibrated reference hydrophone R, followed by

(ii) calibration of the hydrophone H using the (now) calibrated projector P.

In step (i), shown in Fig. 2(a), the modulus of the transmitting response to current $|\underline{S}_{\mathrm{I}}|$ is calculated as

$$|\underline{S}_{\mathrm{I}}| = \frac{d_{\mathrm{PR}}\,U_{\mathrm{R}}}{|\underline{M}_{\mathrm{R}}|\,I_{\mathrm{P}}} = \frac{d_{\mathrm{PR}}\,|\underline{Z}_{\mathrm{PR}}|}{|\underline{M}_{\mathrm{R}}|}, \tag{7}$$

where $|\underline{Z}_{\mathrm{PR}}|$ is the modulus of the electrical transfer impedance between the projector being calibrated P and the calibrated reference hydrophone R, $|\underline{M}_{\mathrm{R}}|$ is the modulus of the calibrated

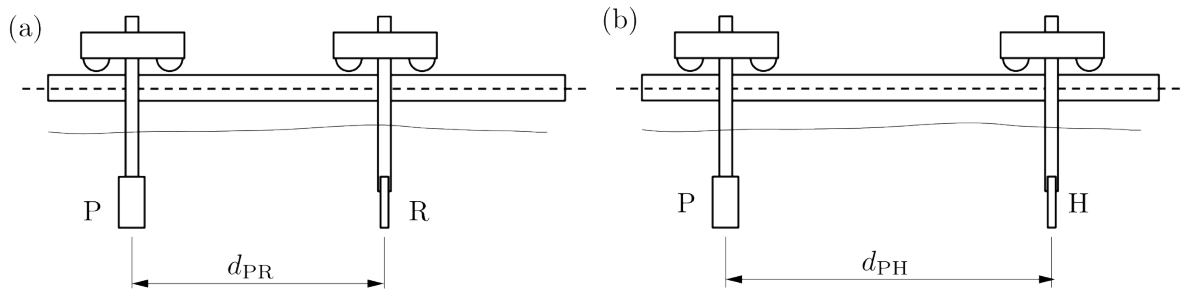

Figure 2: Measurement platform for supporting underwater acoustic transducers: a projector P, a calibrated reference hydrophone R, and a hydrophone to be calibrated H, with separation distances d_{PR} and d_{PH}.

reference hydrophone sensitivity, U_R is the open-circuit voltage output at the reference hydrophone, and I_P is the current supplied to the projector. In step (ii), shown in Fig. 2(b) the reference hydrophone is removed and replaced with the hydrophone to be calibrated, H, yielding the modulus of the hydrophone sensitivity $|\underline{M}_{\mathrm{H}}|$ when ensonified with the by the (now) calibrated projector according to

$$|\underline{M}_{\mathrm{H}}| = \frac{d_{\mathrm{PH}}\, U_{\mathrm{H}}}{|\underline{S}_{\mathrm{I}}|\, I_{\mathrm{P}}} = \frac{d_{\mathrm{PH}}\, |\underline{Z}_{\mathrm{PH}}|}{|\underline{S}_{\mathrm{I}}|}. \tag{8}$$

where $|\underline{Z}_{\mathrm{PH}}|$ is the modulus of the electrical transfer impedance between the calibrated projector P and the hydrophone H, and U_H is the open-circuit voltage output at the hydrophone.

Rearrangement of (7) and (8), yields (9) as the modulus of the free-field sensitivity of the hydrophone being calibrated.

$$|\underline{M}_{\mathrm{H}}| = \frac{d_{\mathrm{PH}}}{d_{\mathrm{PR}}} \frac{|\underline{Z}_{\mathrm{PH}}|}{|\underline{Z}_{\mathrm{PR}}|}\, |\underline{M}_{\mathrm{R}}| \tag{9}$$

The measurement model represented by the combination in (9) can be viewed as calibration of a hydrophone using a calibrated reference hydrophone with collection of the parameter $|Z_{\mathrm{PR}}|$ needed to monitor and control the measurement process. The parameter $|Z_{\mathrm{PR}}|$, measured over frequency, is a good candidate for monitoring the process because it captures the performance of the calibrated projector and reference hydrophone, the electrical measurement system operating them, and the physical setup.

In a high-throughput calibration service, step (i) is performed to measure $|Z_{\mathrm{PR}}|$, which is analyzed as discussed in section 2 to compute the Mahalanobis distance D^2 from the current measurement to the mean value $\boldsymbol{\mu}$ estimated previously using a training data set. The distance D^2 is plotted on a multivariate control chart and compared to the limit T_{u}^2 to verify that the measuring system and calibration process are in-control. Then step (ii) is performed on a customer hydrophone using (8) which is functionally equivalent to (9). This step can be repeated by installing the next customer hydrophone, calibrating as many in a day as demand requires.

Additional process control data can be collected via step (i) at day's end (or any other time) by again measuring the projector-to-reference hydrophone electrical transfer impedance $|Z_{\mathrm{PR}}|$, adding it to the applicable control chart, and confirming that the measuring system and process remain in control. However, experience has shown that this additional measurement does not add much value, except as a means to increase monitoring of a process when its control status is in doubt.

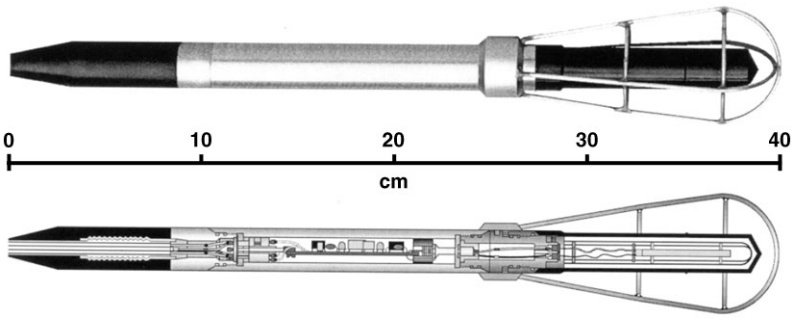

Figure 3: USRD Type H52 hydrophone [10]

4. CASE STUDY

The case study illustrates the use of the process control described in the previous sections. It describes the equipment used to perform free-field relative calibrations in an open water facility at the USRD, the collection of training data to develop process models, the use of the process models to monitor calibrations over a three-month period, and a reference hydrophone failure that was detected by the process control before it would have been noticed by a trained operator.

Calibration services covering the 1 kHz to 200 kHz frequency range require three measuring system configurations, each of which was treated as a distinct process subjected to statistical control. These configurations are distinguished only by the respective projector-amplifier pairings as they all use the the Type H52 reference hydrophone:

- 1 kHz to 10 kHz, ITC-1007 projector, low-band amplifier
- 6 kHz to 50 kHz, Type F83 projector, low-band amplifier
- 40 kHz to 200 kHz, Type F83 projector, high-band amplifier

4.1. TYPE H52 HYDROPHONE BACKGROUND

The Type H52 (Fig. 3) is a wide-band hydrophone used for general purpose underwater acoustic measurements [10] and as a reference measuring standard for relative calibrations in USRD laboratories. The sensing element consists of eight lithium sulfate crystals arranged in a linear array 5-cm long, housed in an oil-filled boot. The nominal operating frequency range spans from 10 Hz to 200 kHz, but is occasionally extended to 250 kHz when required.

When the Type H52 is oriented vertically for use, there is a potential for its response to vary with angle in a vertical plane at higher frequencies and commensurately short wavelengths. A linear aperture of length L (i.e., 5 cm for the Type H52) exhibits a normalized directional response b with respect to angle θ as

$$b(\theta) = \left[\frac{\sin\left(\frac{\pi L}{\lambda}\sin(\theta)\right)}{\frac{\pi L}{\lambda}\sin(\theta)} \right]^2, \tag{10}$$

where λ is the acoustic wavelength [11]. It is expressed in decibels as $10\log_{10}(b)$. Consideration of (10) shows that the directional response is normalized about the angle $\theta = 0$, which corresponds to sound arriving from a direction that is orthogonal to the longitudinal axis of the aperture.

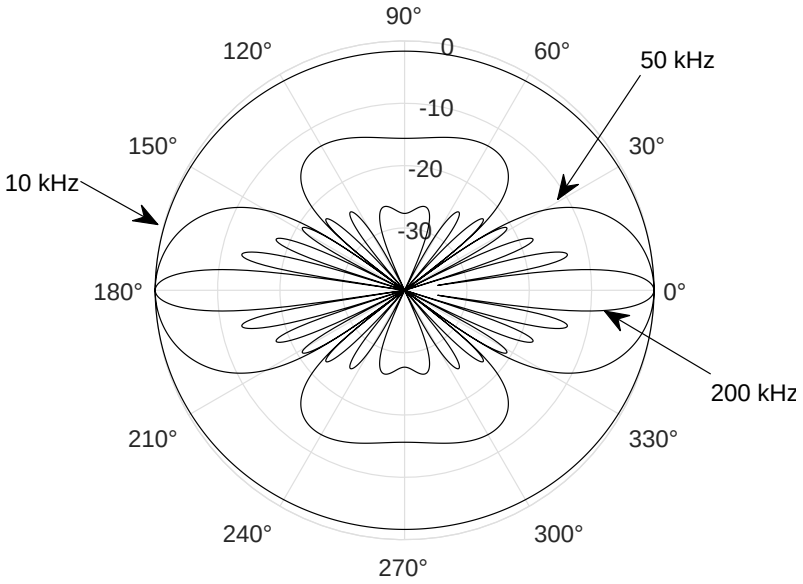

Figure 4: Directional response of the Type H52 hydrophone. The sensitive element is oriented vertically, with its central axis parallel to the $90°$–$270°$ *ordinates. Response with respect to angle in a vertical plane is provided as decibels relative to the sensitivity in the direction of the main response in the horizontal plane for frequencies of 10 kHz, 50 kHz, and 200 kHz. The dynamic range shown in the figure is 40 dB at 10 dB per division. A nominal sound speed of 1500 m/s was assumed.*

Fig. 4 shows the directional response, or *beam pattern*, for the Type H52 hydrophone at 10 kHz, 50 kHz and 200 kHz. As shown in the figure, the angular width of the hydrophone's main response becomes more narrow as frequency is increased. As a result, the potential for measurement errors due to misalignment or unintended vertical displacement of the sensitive element increases with frequency.

4.2. COLLECTION AND PROCESSING OF TRAINING DATA

Training data were collected from August through October, 2019 and subsequently analyzed to yield the estimated mean vector $\hat{\boldsymbol{\mu}}$ and covariance matrix $\hat{\mathbf{C}}$ for the electrical transfer impedance $|Z_{\mathrm{PR}}|$ between each projector and a Type H52 calibrated reference hydrophone. In all cases, about 35 transfer impedance measurements were performed across each respective frequency band. Outliers were removed as described in section 2 using (5) to establish the threshold for data objects to be removed from the training data. At the conclusion of this process, the number of observations remaining in the training data ranged from 25 to 31.

Following removal of outliers, the mean vector $\hat{\boldsymbol{\mu}}$ and covariance matrix $\hat{\mathbf{C}}$ were computed for each projector-amplifier pairing. The upper control limit T_{u}^2 for each control chart was calculated using (6).

4.3. COLLECTION AND PROCESSING OF OPERATING DATA

Monitoring and control of free-field calibration services using training data to verify the control status of the measuring system and process began in December, 2019. The electrical transfer

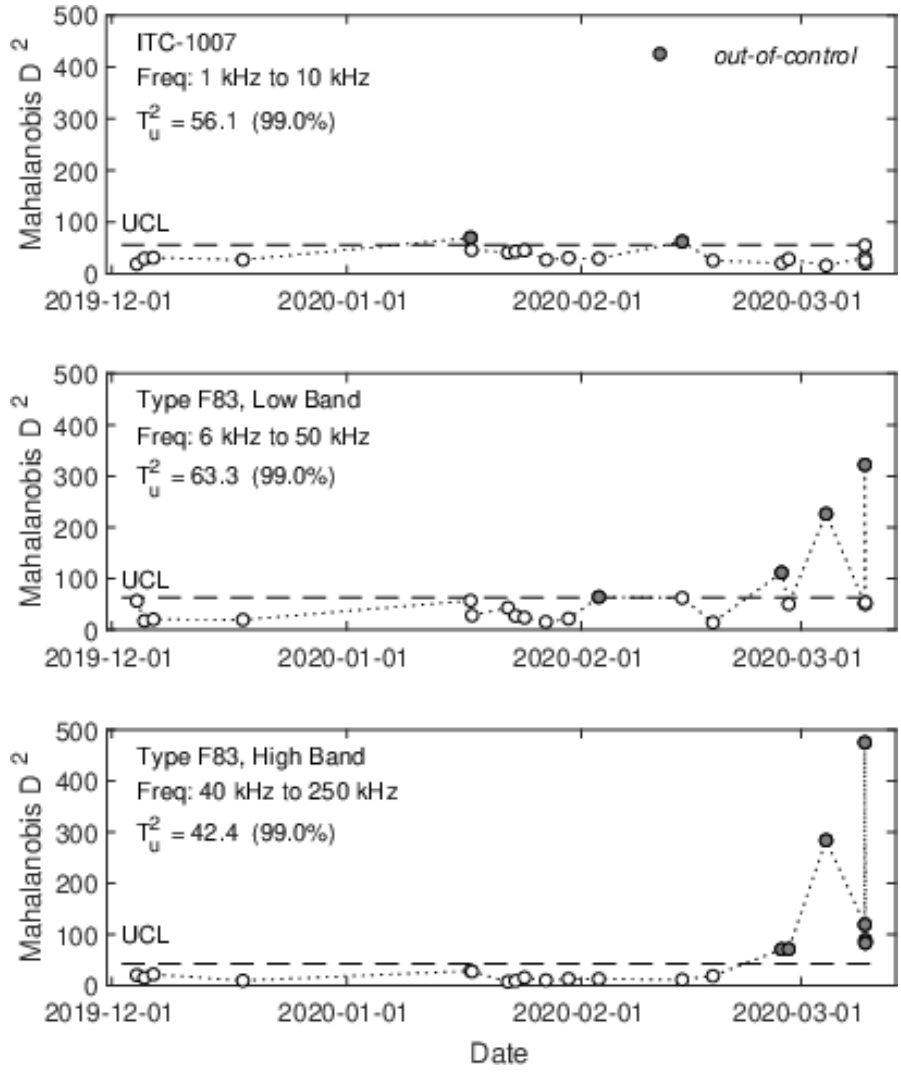

Figure 5: Multivariate control charts for electrical transfer impedance between two different acoustic projectors and a Type H52 calibrated reference hydrophone. The upper control limit (UCL) was computed as T_u^2 for a critical value of 0.99 and annotated on each chart. Calibration service was halted on 9 March 2020 to initiate a root-cause investigation.

impedance $|Z_{\mathrm{PR}}|$ was measured at the start of each day that the laboratory was scheduled to perform relative calibrations of hydrophones. The distance D^2 of each impedance measurement from the mean vector $\hat{\boldsymbol{\mu}}$ was compared to its respective control limit T_{u}^2.

Fig. 5 shows control charts for this calibration service starting in December, 2019 and continuing through March, 2020. Each subplot depicts the control data for a different projector-amplifier pairing, which is annotated in the respective control chart. A single Type H52 calibrated reference hydrophone was used for all cases. The frequency band spanned by each measurement, and the associated control threshold T_{u}^2 are annotated on each chart. Control limits were computed using (6) for a critical value $\alpha = 0.99$ in all cases. Markers for impedance measurements in which the control limit was exceeded ($D_i^2 > T_{\mathrm{u}}^2$) are filled as annotated in the legend.

Electrical transfer impedance measurements $|Z_{\mathrm{PR}}|$ remained in control until late-February, when measurements performed with the Type F83 projector began to exceed the control limit

T_u^2. Since misalignment between projector and hydrophone can be a common, and easily corrected, cause for calibration errors, attempts were made to remove and realign the acoustic transducers. As the lower two control charts in Fig. 5 show, the distance D^2 was significantly reduced only to increase again with the process trending rapidly toward out-of-control conditions of increasing severity. Calibration services were paused on 9 March, 2020 to perform a root-cause investigation.

The root-cause investigation explored several potential issues with the measuring system and process that could explain the problematic electrical transfer impedance measurements. Among the actions taken was disassembly and inspection of the Type H52 calibrated reference hydrophone. Upon removal of the protective rubber boot (see Fig. 3), it was discovered that the lithium sulfate crystal array had become dislodged from its mount, freeing it to move within its oil-filled volume. With the sensitive element insufficiently constrained, relatively small angular displacements resulted in a loss of control for the alignment of the hydrophone's main response axis. Consideration of Fig. 4 confirms that a relatively small angular misalignment of the sensitive element will cause the electrical transfer impedance measurement Z_{PR} to change and that the relative magnitude of that change will increase with frequency as depicted in Fig. 5.

The affected Type H52 hydrophone was withdrawn from service pending repair and replaced with another of the same model. After collection of a new training data set, the process was reestablished and remained in control.

5. CONCLUSION

Calibration laboratories that perform to the requirements of [1] are obligated to collect and analyze data to help ensure the validity of their measurements. Among the desirable characteristics for an effective process control are: 1) the analysis provides timely and accurate information about the monitored process, 2) the analysis yields an objective result that can be cited in the laboratory's quality procedures and used to initiate corrective action, 3) data subjected to analysis are produced naturally by the process being monitored, 4) the analysis procedure is efficient, or preferably, automated, and 5) the analysis result can be interpreted and acted upon by laboratory personnel without extensive training in statistical methods.

When developing a system of statistical controls for its free-field calibration services, the USRD adapted methods common to the chemical process industry. Such techniques allow for a large number of different, and potentially correlated, parameters to be analyzed together within a multivariate probability distribution, that describes the state of the process using a single value, the Mahalanobis distance. This distance can be plotted in a Shewhart-like control chart with a well-defined control limit.

In the USRD application, the process control operates on multivariate data generated naturally by the calibration procedure (i.e., the electrical transfer impedance), and that the monitored process operates according to a known model that relates the electrical transfer impedance data to product quality and the consistency of the end-to-end test setup over time. A case study using this method showed that it is sensitive to small changes in the test setup, like emerging degradation in a reference hydrophone, alerting the operator before the change would be otherwise apparent in the calibration results.

6. ACKNOWLEDGMENTS

This work was supported by funding from the Naval Undersea Warfare Center's Underwater Sound Reference Division (NUWC-USRD). The enthusiastic support of Mr. Anthony Paolero is gratefully acknowledged. Ms. Kari Harper, of the National Voluntary Laboratory Accreditation Program (NVLAP), provided valuable assessments of the laboratory's activities, including helpful guidance as these statistical methods were developed, deployed and validated. Finally, the authors are indebted to technical staff at the NUWC-USRD Open Tank Facility (OTF). Their hard work was essential to the development, evaluation and success of these control procedures.

REFERENCES

[1] "General requirements for the competence of testing and calibration laboratories," ISO/IEC 17025:2017, International Standards Organization, International Electrotechnical Commission, Geneva, CH, 2017.

[2] W. A. Shewhart, *Economic control of quality of manufactured product*. New York, NY: D. Van Nostrand Company, 1931.

[3] T. Kourti and J. F. MacGregor, "Process analysis, monitoring and diagnosis, using multivariate projection methods," *Chemometrics and Intelligent Laboratory Systems*, vol. 28, no. 1, pp. 3–21, 1995.

[4] O. Mestek, J. Pavlik, and M. Suchánek, "Multivariate control charts: Control charts for calibration curves," *Fresenius' Journal of Analytical Chemistry*, vol. 350, no. 6, pp. 344–351, 1994.

[5] P. C. Mahalanobis, "On the generalized distance in statistics," *Proceedings of the National Institute of Science of India*, vol. 12, pp. 49–55, 1936.

[6] "Underwater acoustics – Hydrophones – Calibration of hydrophones – Part 1: Procedures for free-field calibration of hydrophones," IEC 60565-1:2020, International Electrotechnical Commission, Geneva, CH, 2020.

[7] B. MacCarthy and T. Wasusri, "A review of non-standard applications of statistical process control (SPC) charts," *International Journal of Quality & Reliability Management*, vol. 19, no. 3, pp. 295–320, 2002.

[8] R. De Maesschalck, D. Jouan Rimbaud, and D. L. Massart, "The Mahalanobis distance," *Chemometrics and Intelligent Laboratory Systems*, vol. 50, no. 1, pp. 1–18, 2000.

[9] A. R. Mukhopadhyay, "Multivariate attribute control chart using Mahalanobis D^2 statistic," *Journal of Applied Statistics*, vol. 35, no. 4, pp. 421–429, 2008.

[10] A. L. Van Buren, R. M. Drake, and A. E. Paolero, "Temperature dependence of the sensitivity of hydrophone standards used in international comparisons," *Metrologia*, vol. 36, no. 4, pp. 281–285, 1999.

[11] R. J. Urick, *Principles of Underwater Sound*. New York, NY: McGraw-Hill Book Company, 3rd ed., 1984.